Effect of Passivation and Mechanical Constraint on Electromigration in Interconnect

Cui, Zhen; Fan, Xuejun; Zhang, Guoqi

DOI
10.1109/ECTC51909.2023.00226

Publication date
2023

Document Version
Final published version

Published in
Proceedings of the 2023 IEEE 73rd Electronic Components and Technology Conference (ECTC)

Effect of Passivation and Mechanical Constraint on Electromigration in Interconnect

Zhen Cui
Delft University of Technology
Delft, Netherlands
z.cui@tudelft.nl

Xuejun Fan
Lamar University
Beaumont, TX 77710, USA
xuejun.fan@lamar.edu

Guoqi Zhang
Delft University of Technology
Delft, Netherlands
g.q.zhang@tudelft.nl

***Abstract*—In this paper, we apply the Eshelby's solution to study the effect of passivation layer on electromigration (EM) failure in a conductor. The passivation layer is considered as an elastic material, not a rigid layer anymore. Thus, the deformation and stress evolution in the conductor during EM are related to the mechanical property of the passivation layer. One-dimensional (1D) analytical solution for the passivated conductor is obtained. The numerical results show that the conductor covered with the stiffer passivation layer has much less EM damage. And the steady-state solution shows that the magnitude of (jL)c increases with increasing Young's modulus of passivation material. The present study provides a way to predict the EM performances taking into account various passivation materials.**

Keywords—electromigration; coupling theory; passivation; Eshelby's solution.

I. Introduction

Electromigration (EM) is a mass transport process in metal interconnects induced by high electrical current density, which causes material depletions near the cathode side and material accumulations near the anode side, resulting in opens or shorts in microelectronic devices. [1-5] With the continued scaling down of interconnect technology, EM is one of the critical challenges for the reliability of interconnects [6-8].

Covering the metal conductor with a dielectric material is an effective way to reduce EM damage. In pure metals, atoms exchange place with vacancies and travel from cathode towards the anode of the conductor during EM [9-12]. The depletions of atoms will lead to a local volume contraction. In turn, the accumulations of atoms will produce a local volume expansion. When the conductor is constrained by the dielectric materials, these volume changes due to mass transport will induce a mechanical stress gradient.

In the experimental study, Blech et al. [13-15] found that covering SiN on Al line could increase the critical conductor length and decrease the drift velocity of EM. Lloyd and Smith [10] found that the EM lifetime of aluminum conductors changes as a function of passivation thickness. The conductors covered with thicker glass lasted longer than those conductors with thin glass or without glass in terms of EM-induced damage. And all uncovered conductors and conductors covered with thin glass failed by open circuit due to void formation, whereas those with thick glass failed by short circuit due to hillock formation. Moreover, in the study done by Wada et al. [2], it was found that the lifetime of Al line with SiN passivation layer is longer than that with SiO_2 passivation layer. Authors believed that this is because a larger mechanical strength of the SiN layer can better inhibit the growth of hillocks due to EM, compared to the SiO_2 layer.

Korhonen et al. [16] considered that the Al line was embedded in a rigid layer and assumed that the Al line was constrained everywhere. As discussed in the paper [15], an over-estimated hydrostatic stress was obtained using Korhonen's model. Sarychev et al. [17] and Sukharev et al. [18, 19] developed new EM models, but both works still used the same incorrect mechanical boundary conditions. The impact of passivation on stress evolution during EM was ignored. Recently, Cui et al. developed a general coupling model [20] and proposed a diffusion-indued strain [21]. Authors correctly considered the mechanical constraints for a fully fixed conductor, and numerical results showed that the development of EM in the fully confined conductor is slower than that in the bare conductor. And the predicted threshold product in a confined conductor is larger than that in a bare conductor, which is consistent with Blech's experimental results. We have used different software such as ANSYS and COMSOL, and different numerical approaches, such as peridynamics and finite element method to obtain the numerical solutions.[22-25]

In this paper, EM in the passivated conductor is further studied on the basis of the coupling theory. The passivation layer is considered as an elastic material, not the rigid layer anymore. Eshelby's solution is used to describe the stress-strain relationship. The obtained results are compared with previous results for conductors under stress-free and fully fixed conditions. According to the steady-state solutions and critical atomic concentration for EM failure, the threshold product of current density and conductor length (jL)c is determined as a function of the Young's modulus of passivation layer.

II. Theory

A. One-Dimensional Coupling Theory

Based on the general coupling model presented in the paper [20] and diffusion-induced strain developed in the paper [21], a fully-coupled EM theory was proposed.[7] Here, the 1D formulations of the coupling theory are introduced. Mass conservation equation is used to describe the EM (see Eq. (1)), in which θ is the total volumetric strain, and J_a is the total atomic flux,

2023 IEEE 73rd Electronic Components and Technology Conference (ECTC) | 979-8-3503-3498-2/23/$31.00 ©2023 IEEE | DOI: 10.1109/ECTC51909.2023.00226

2377-5726/23/$31.00 ©2023 IEEE
DOI 10.1109/ECTC51909.2023.00226

$$\frac{\partial \theta}{\partial t} = -\Omega \nabla \cdot J_a \tag{1}$$

As the present study focuses on the impact of mechanical constraints on EM, thus the atomic flux driven by temperature gradient was neglected. The total atomic flux is given as follows,[26-28]

$$J_a = D_a\left(-\frac{\partial C_a}{\partial x} - \frac{Z^* e\rho j}{k_B T} C_a + \frac{C_a \Omega}{k_B T}\frac{\partial \sigma}{\partial x}\right) \tag{2}$$

where D_a is the atomic diffusivity, j is the current density, e is the elementary charge, ρ is the electrical resistance, Z^* is the effective charge number ($Z^* > 0$) [29], and σ is the hydrostatic stress.

Despite 1D assumption, 3D constitutive equation must be applied to obtain the stress and strain. The total volumetric strain θ in Eq. (1) and hydrostatic stress σ in Eq. (2) are,

$$\theta = \varepsilon_x + \varepsilon_y + \varepsilon_z \tag{3}$$

$$\sigma = \frac{1}{3}(\sigma_x + \sigma_y + \sigma_z) \tag{4}$$

Considering that the material is linearly elastic and isotropic, the stress-strain relation is described based on Hooke's law as follows:

$$\sigma = 2G\varepsilon + \lambda tr(\varepsilon)\boldsymbol{I} - Btr(\varepsilon^{\text{diff}})\boldsymbol{I} \tag{5}$$

where G and λ are Lamé constants, $2G=E/(1+\upsilon)$ and $\lambda = 2G\upsilon/(1-2\upsilon)$, E is the Young's modulus, υ is the Poisson's ratio, $B = \lambda + 2G/3$ is the bulk modulus. And the $\boldsymbol{\varepsilon}^{\text{diff}}$ is [21]

$$\boldsymbol{\varepsilon}^{\text{diff}} = \int_{C_{a0}}^{C_a} \frac{(1-f)}{3}\frac{dC_a}{C_a}\boldsymbol{I} \tag{6}$$

where f is the vacancy relaxation factor.

Moreover, the mass conservation equation was coupled with the 1D stress equilibrium equation as follows:

$$\frac{\partial \sigma_x}{\partial x} = 0 \tag{7}$$

B. Eshelby's solution

For a conductor passivated by dielectric, the eigenstrains of the conductor, e.g., thermal strain and diffusion strain, induce mechanical stress and affect total strain in the conductor. The classical Eshelby's solution gives an analytical relation between total strain and imposed eigenstrain as follows,[30]

$$\boldsymbol{\varepsilon} = S\boldsymbol{\varepsilon}^* \tag{8}$$

where S is the Eshelby's tensor, and $\boldsymbol{\varepsilon}^*$ is the eigenstrain. In the refer. [7], we equalized the passivated conductor with diffusion-induced strain as a plane-stress inhomogeneity Eshelby inclusion problem. Here we directly give the relationship between total strain and diffusion-induced strain in the conductor as follows,

$$\varepsilon_x = \frac{(1+v_c)(1-2v_c)+\varphi\,(1+v_m)}{E_c(1+\varphi-v_c+\varphi v_m)}\sigma_x + \frac{1+\varphi+\varphi v_m+v_c}{1+\varphi+\varphi v_m-v_c}\varepsilon^{\text{diff}} \tag{9}$$

$$\varepsilon_y = \varepsilon_z = \frac{(1+v_m)\varphi}{1-v_c+\varphi+\varphi v_m}\left(\varepsilon^{\text{diff}} - \frac{v_c\sigma_x}{E_c}\right) \tag{10}$$

where E_c and v_c are the Young's modulus and Poisson's ratio of the conductor, respectively. E_m and v_m are the Young's modulus and Poisson's ratio of passivation material, respectively. φ is the ratio of E_c to E_m ($\varphi=E_c/E_m$).

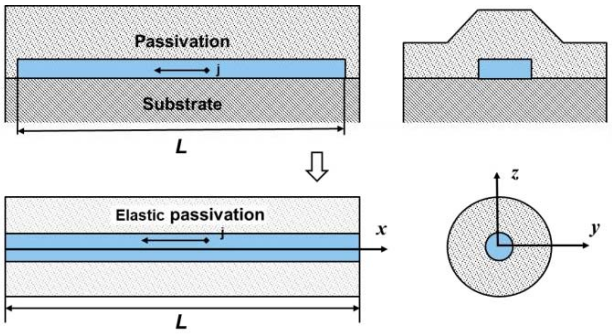

Fig. 1 Schematic of the passivated conductor. The conductor was idealized as a cylindrical shape, which is passivated by an elastic material.

III. One Dimensional Solutions

A. Governing equation for passivated conductor

Let us consider a 1D problem for the conductor passivated by an elastic dielectric. To obtain an approximate solution, the conductor line was idealized as a cylindrical shape, shown in Fig. 2. The cylinder was laterally passivated by elastic material, and both ends were constrained.

Thus,

$$u_x(0) = u_x(L) = 0 \tag{11}$$

Eq. (11) actually means that the total integral of strain in the x-direction is zero,

$$\int_0^L \varepsilon_x\, dx = 0 \tag{12}$$

Moreover, based on the 1D equilibrium equation, the σ_x keeps constant along conductor length,

$$\frac{d\sigma_x}{dx} = 0 \;\rightarrow\; \sigma_x = \sigma_0 \tag{13}$$

Applying Equations (12) and (13) to Eq (9), we can obtain σ_x as follows,

$$\sigma_x = -\frac{E_c(1+\varphi+\varphi v_m+v_c)}{[(1+v_c)(1-2v_c)+\varphi(1+v_m)]L}\int_0^L \varepsilon^{\text{diff}} dx \tag{14}$$

Then, using Eq. (14) in Eqs. (5) and (10), the following strains and stresses can be determined,

$$\sigma_y = \sigma_z$$
$$= -\frac{E_c}{1-v_c+\varphi+\varphi v_m}(\varepsilon^{\text{diff}} + \frac{v_c(1+v_c+\varphi+\varphi v_m)}{[(1+v_c)(1-2v_c)+\varphi(1+v_m)]L}\int_0^L \varepsilon^{\text{diff}} dx) \quad (15)$$

Finally, the following governing equations for atomic concentration and hydrostatic stress are obtained as follows:

$$\frac{1+v_c+3(1+v_m)\varphi}{3(1-v_c+\varphi+\varphi v_m)}\frac{1-f}{C_a}\frac{\partial C_a}{\partial t} - \frac{(1+v_c+\varphi+\varphi v_m)^2}{3[(1+v_c)(1-2v_c)+\varphi(1+v_m)]} \frac{(1-2v_c)}{(1-v_c+\varphi+\varphi v_m)L}\int_0^L \frac{1-f}{C_a}\frac{\partial C_a}{\partial t}$$
$$= D_a\{-\frac{Z^* e\rho j}{k_B T}\frac{\partial C_a}{\partial x} + \frac{\partial^2 C_a}{\partial x^2} + \frac{2E_c\Omega}{9(1-v_c+\varphi+\varphi v_m)k_B T}[(1-f)\frac{\partial^2 C_a}{\partial x^2} - \frac{\partial f}{\partial C_a}\left(\frac{\partial C_a}{\partial x}\right)^2]\} \quad (16)$$

$$\sigma = -\frac{2E_c}{9(1-v_c+\varphi(1+v_m))}[\int_{C_{a0}}^{C_a}\frac{1-f}{C_a}dC_a + \frac{(1+v_c+\varphi+\varphi v_m)^2\int_0^L\int_{C_{a0}}^{C_a}\frac{1-f}{C_a}dC_a dx}{2[(1+v_c)(1-2v_c)+\varphi(1+v_m)]L}] \quad (17)$$

As the atomic flux is blocked at both ends, thus,

$$\frac{Z^* e\rho j}{k_B T}C_a(0,\,t) - [1+\frac{2E_c(1-f)}{9[1-v_c+\varphi+\varphi v_m]}\frac{\Omega}{k_B T}]\frac{\partial C_a(0,\,t)}{\partial x} = 0 \quad (18)$$

$$\frac{Z^* e\rho j}{k_B T}C_a(L,\,t) - [1+\frac{2E_c(1-f)}{9[1-v_c+\varphi+\varphi v_m]}\frac{\Omega}{k_B T}]\frac{\partial C_a(L,\,t)}{\partial x} = 0 \quad (19)$$

Atomic concentration $C_a(x,t)$ and hydrostatic stress $\sigma(x,t)$ are two coupled variables to be solved. And we assume that the EM failure takes place when the atomic concentration $C_a(x,t)$ decreases to its critical value $C_{a,\text{critical}}$.

B. Steady-state solution

At the steady state, Eq. (16) becomes,

$$-\frac{Z^* e\rho j}{k_B T}\frac{\partial C_a}{\partial x} + \frac{\partial^2 C_a}{\partial x^2} + \frac{2E_c\Omega}{9(1-v_c+\varphi+\varphi v_m)k_B T}[(1-f)\frac{\partial^2 C_a}{\partial x^2} - \frac{\partial f}{\partial C_a}\left(\frac{\partial C_a}{\partial x}\right)^2] = 0 \quad (20)$$

Solving Eq. (20), we obtain the following equation,

$$jL = \frac{k_B T}{Z^* e\rho}\left[1+\frac{2E_c(1-f)\Omega}{9[1-v_c+(1+v_m)\varphi]k_B T}\right]\ln[\frac{C_{a,x=L}}{C_{a,x=0}}] \quad (21)$$

When C_a at cathode (x=0) reaches the critical atomic concentration, we have,

$$C_{a,x=0} = C_{a,\text{critical}} \quad (22)$$

$$C_{a,x=L} = C_{a0} + (C_{a0} - C_{a,\text{critical}}) = 2C_{a0} - C_{a,\text{critical}} \quad (23)$$

Applying above critical conditions in Eq. (21), we can obtain the threshold product of current density and conductor length as follows,

$$(JL)_c = \frac{k_B T}{Z^* e\rho}\left[1+\frac{2E_c(1-f)\Omega}{9[1-v_c+(1+v_m)\varphi]k_B T}\right]\ln(\frac{2C_{a0}}{C_{a,\text{critcial}}}-1) \quad (24)$$

We have defined $C_{a,\text{critical}}$ as a material property. Thus, the magnitude of threshold product for a conductor depends on the value of φ.

IV. Results and Discussion

The properties of the metal line are listed in Table. 1. Vacancy relaxation factor (f) as a function of C_a is given in Eq. (26). [21]

Table 1. Material properties

Young's modulus (E_c)	70 GPa
Poisson ratio (v_c)	0.33
Atomic diffusivity (D_a)	1×10^{-14} m^2/s
Atomic volume (Ω)	1.66×10^{-29} m^3
Electrical resistivity (ρ)	2.88×10^{-8} Ohm·m
Current density (j)	1×10^{10} A/m^2
Elementary charge (e)	1.6×10^{-19} C
Charge number (Z^*)	1.1
Bolzmann constant (k_B)	1.38×10^{-23} J/K

$$f=\begin{cases}0.73, & |C_a-C_{a0}|<0.0075\\ 1.08\exp\left(-55.3\left|1-\dfrac{C_a}{C_{a0}}\right|\right), & |C_a-C_{a0}|>0.0075\end{cases} \quad (25)$$

Fig. 2(a) shows the distributions of the normalized atom concentrations (C_a/C_{a0}) for 200 μm passivated conductor with E_m=140 GPa and un-passivated conductor at different times: 1000s, 5000s, and 10000s. The analytical solution for the un-passivated conductor is the same as Eq. (17) when we set E_m=0. At cathode side, C_a in passivated conductor decreases slower than C_a in conductor without passivation. At the anode side, the passivated conductor has lower C_a than the un-passivated conductor. It means that the EM is significantly reduced in passivated conductor. Correspondingly, the distributions of hydrostatic stress in both conductors are plotted in Fig. 2(b). Without passivation, stress along the conductor at all times keeps zero. With passivation, the tensile hydrostatic stress generates at the cathode side due to the depletion of atoms, and the compressive hydrostatic stress forms at the anode due to the accumulation of atoms. The direction of gradient of hydrostatic stress is opposite to the direction of EM, which plays a role in resisting EM.

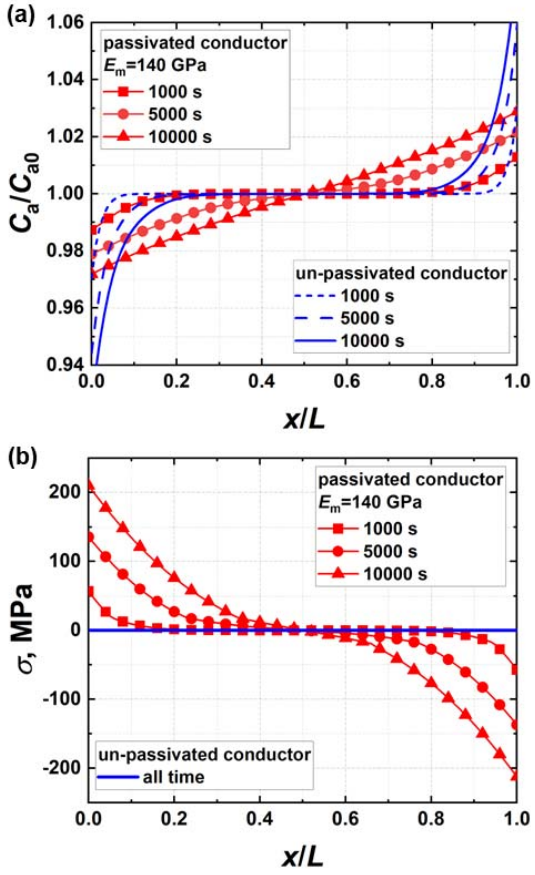

Fig. 2. (a) Distributions of atomic concentrations along 200 μm passivated and un-passivated Al line under a current density of 1 MA/cm^2 at various times. (b) Distributions of hydrostatic stress along 200 μm passivated and un-passivated Al line under a current density of 1 MA/cm2 at various times.

For the passivated conductor, the material property of passivation affects EM. Fig. 3(a) plots the evolution of atomic concentration at cathode side over time in conductor when the passivation layer has various magnitudes of Young's modulus. C_a decreases slower with larger Young's modulus of passivation layer. It indicates that stiffer passivation has better performance in reducing EM. These simulation results are consistent with some experimental results [10, 12]. It is because that, under the same current loading, a larger mechanical stress can be reached in the conductor with stiffer passivation, as the results shown in Fig. 3(b).

The threshold product $(jL)_c$ is determined as a function of E_m using Eq. (25) after knowing $C_{a,critical}$=0.96 C_{a0} for annealed Al. Please see refer. [7] for the method to determine critical atomic concentration. Fig. 4 shows that the magnitudes of threshold product $(jL)_c$ increase from 10^3 A/cm to 5×10^4 A/cm with increasing E_m from 0 to 500 GPa. It means that the conductor with and without passivation significantly affects critical conductor length or maximum current density. Moreover, the threshold product for fully fixed conductor is obviously higher than those results when the passivation is considered as elastic material. It means that if we consider the passivation layers SiO_2 with E_m= 70 GPa or SiN with E_m=140 GPa as fully constrained condition on conductors, it will cause over-estimated results.

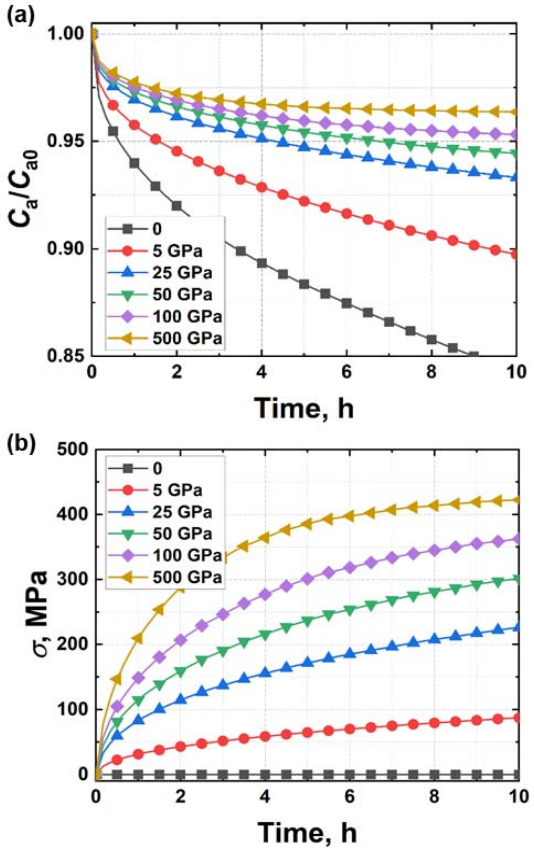

Fig. 3. (a) Evolutions of atomic concentrations and (b) evolutions of hydrostatic stress at cathode side for the conductor covered by passivation layer with various Young's modulus under a current density of 1 MA/cm^2.

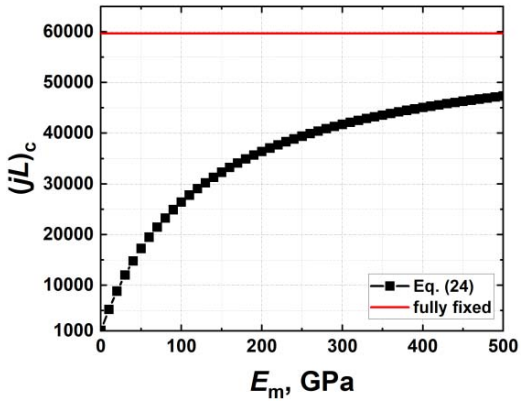

Fig. 4. Predicted threshold products $jL = (jL)_c$ curves for Al covered by passivation with E_m changing from 0 to 500 GPa.

V. CONCLUSION

In this paper, we obtained the 1D analytical solution for EM development in the conductor with the consideration of the mechanical property of passivation material. The numerical results showed that the EM develops slower in the conductor covered with stiffer passivation layer. And the steady-state solution showed that the magnitude of $(jL)_c$ increases with increasing Young's modulus of passivation material. These results are consistent with experimental results in the literature. The present study provides a way to predict the EM performances taking into account various passivation materials.

REFERENCES

1. Tan, C.M. and A. Roy, *Electromigration in ULSI interconnects.* Materials Science & Engineering R, 2007. **58**(1-2): p. 1-75.
2. Wang, P.-C. and R. Filippi, *Electromigration threshold in copper interconnects.* Applied Physics Letters, 2001. **78**(23): p. 3598-3600.
3. Ho, P.S. and T. Kwok, *Electromigration in metals.* Reports on Progress in Physics, 1989. **52**(3): p. 301.
4. Fan, X., *New Results on Electromigration Modeling in Microelectronics*. 2019: Electronic Packaging Society (EPS) Webinar.
5. Dandu, P. and X. Fan. *Assessment of current density singularity in electromigration of solder bumps*. in *2011 IEEE 61st Electronic Components and Technology Conference (ECTC)*. 2011.
6. Kijkanjanapaiboon, K., *Modeling of Electromigration and Lock-in Thermography in Micro-electronics Packaging.* Doctoral Dissertation, 2017.
7. Cui, Z., *Multi-Physics driven electromigration study: multi-scale modeling and experiment*. 2021, PhD. Dissertation, Delft University of Technology.
8. Ma, R., et al. *Electromigration simulation of flip chip CSP LED*. in *2017 18th International Conference on Electronic Packaging Technology (ICEPT)*. 2017. IEEE.
9. Kimura, Y., et al., *Suitable passivation thickness on a metal line to prevent electromigration damage.* Materials Letters, 2016. **184**(DEC.1): p. 219-222.
10. Lloyd, J. and P. Smith, *The effect of passivation thickness on the electromigration lifetime of Al/Cu thin film conductors.* Journal of Vacuum Science & Technology A: Vacuum, Surfaces, and Films, 1983. **1**(2): p. 455-458.
11. Lloyd, J., P. Smith, and G. Prokop, *The role of metal and passivation defects in electromigration-induced damage in thin film conductors.* Thin Solid Films, 1982. **93**(3-4): p. 385-395.
12. Wada, T., M. Sugimoto, and T. Ajiki, *The influence of passivation and packaging on electromigration.* Solid-state electronics, 1987. **30**(5): p. 493-496.
13. Blech, I. and C. Herring, *Stress generation by electromigration.* Applied Physics Letters, 1976. **29**(3): p. 131-133.
14. Blech, I. and E. Meieran, *Electromigration in thin Al films.* Journal of Applied Physics, 1969. **40**(2): p. 485-491.
15. Blech, I.A., *Electromigration in thin aluminum films on titanium nitride.* Journal of applied physics, 1976. **47**(4): p. 1203-1208.
16. Korhonen, M.A., et al., *Stress evolution due to electromigration in confined metal lines.* Journal of Applied Physics, 1993. **73**(8): p. 3790-3799.
17. Sarychev, M.E. and Y.V. Zhitnikov, *General model for mechanical stress evolution during electromigration.* Thin Solid Films, 1999. **86**(6): p. 3068-3075.
18. Sukharev, V. and E. Zschech, *A model for electromigration-induced degradation mechanisms in dual-inlaid copper interconnects: Effect of interface bonding strength.* Journal of Applied Physics, 2004. **96**(11): p. 6337-6343.
19. Sukharev, V., E. Zschech, and W.D. Nix, *A model for electromigration-induced degradation mechanisms in dual-inlaid copper interconnects: Effect of microstructure.* Journal of Applied Physics, 2007. **102**(5): p. 053505.
20. Cui, Z., X. Fan, and G. Zhang, *General coupling model for electromigration and one-dimensional numerical solutions.* Journal of Applied Physics, 2019. **125**(10): p. 105101.
21. Cui, Z., X. Fan, and G. Zhang, *Molecular dynamic study for concentration-dependent volume relaxation of vacancy.* Microelectronics Reliability, 2021. **120**: p. 114127.
22. Cui, Z., X. Fan, and G. Zhang. *Implementation of Fully Coupled Electromigration Theory in COMSOL*. in *2022 IEEE 72nd Electronic Components and Technology Conference (ECTC)*. 2022. IEEE.
23. Cui, Z., X. Fan, and G. Zhang. *Implementation of General Coupling Model of Electromigration in ANSYS. 2020 IEEE 70th Electronic Components and Technology Conference (ECTC)*. 2020. IEEE.
24. Taner, O., K. Kijkanjanapaiboon, and X. Fan. *Does current crowding induce vacancy concentration singularity in electromigration?* in *2014 IEEE 64th Electronic Components and Technology Conference (ECTC)*. 2014. IEEE.
25. Y. Zhang, et al., *Fully Coupled Electromigration Modeling Using Peridynamics*, in *2023 IEEE 73nd Electronic Components and Technology Conference (ECTC).* 2023.
26. Dandu, P., et al., *Finite element modeling on electromigration of solder joints in wafer level packages.* Microelectronics Reliability, 2010. **50**(4): p. 547-555.
27. Dandu, P., X.J. Fan, and Y. Liu. *Some remarks on finite element modeling of electromigration in solder joints*. in *Electronic Components & Technology Conference*. 2010.
28. Zhang, Y., et al., *The effect of atomic density gradient in electromigration.* International Journal of Materials & Structural Integrity, 2012. **6**(1): p. 36-53.
29. Fan, X. and Y. Liu, *Design, reliability and electromigration in chip scale wafer level packaging.* ECTC professional development short course notes, 2009.
30. Mura, T., *Inclusion problems.* 1988.